Available online at www.dergipark.org.tr/en

INTERNATIONAL ADVANCED RESEARCHES and ENGINEERING JOURNAL

Journal homepage: www.dergipark.org.tr/en/pub/iarej

e-ISSN: 2618-575X

International Open Access

Volume 06
Issue 02

August, 2022

Research Article

Examining the hydrophobic properties of electrospun oxide-induced polystyrene nanofibers for application in oil-water separation

Kemal Doğan [a,*], ***Ali Akbar Hussaini*** [b], ***Mehmet Okan Erdal*** [c,*] ***and Murat Yıldırım*** [b]

[a]*Selcuk University, Institute of Science, Department of Nanotechnology and Advanced Materials, Konya, 42130, Turkey*
[b]*Selçuk University, Faculty of Science, Department of Biotechnology, Konya, 42130, Turkey*
[c]*Necmettin Erbakan University, Meram Vocational School, Konya, 42090, Turkey*

ARTICLE INFO

Article history:
Received 17 February 2022
Accepted 21 June 2022
Published 15 August 2022

Keywords:
Nanofiber
Polystyrene
Water-oil separation

ABSTRACT

Nanofibers have great importance in the membrane technology used in hydrophobic surface filtration studies applied to water-oil separation products. This study improves upon the hydrophobic properties of electrospun polystyrene-based nanofibers by increasing surface contact angles. As a result, nanofibers have been produced by adding ZnO, MoO_3, NiO, SiO_2, and TiO_2 additives to the polystyrene (PS)/dimethylformamide (DMF) polymer solution at 5% of the mass. Surface contact angle (CA), fourier-transform infrared spectroscopy (FTIR), and scanning electron microscope (SEM) images of the nanofibers were taken. The obtained results were evaluated and show the fiber diameter to range from 555 to 1553 nm. The addition process was observed to be able to affect the polystyrene fiber's ability to retain water. Moreover, surface contact angle of polystyrene increased to 143° by TiO_2 addition. Furthermore, the highest oil-carrying capacity is concluded to have been observed on the SiO_2 and MoO_3 doped fibers.

1. Introduction

Oil plays a vital role in the modern industrial world. Despite being a necessary raw material for a variety of chemical and synthetic polymer fabrications, it is not found in all regions of the world. Moreover, undesirable accidents occur while processing it, such as in its transportation, usage, and storage. This causes not only a loss of energy but also threatens the environment [1]. Accidents in crude oil transportation have created undeniable catastrophes requiring clean-up operations, with 5,000 tons of oil spilled annually between 2010–2014 [2]. The most noteworthy examples of major accidents have been the Torrey Canyon (1967), Amoco Cadiz (1978), Atlantic Empress (1979), Exxon Valdez (1990), and ABT Summer (1991) spills that resulted in major environmental impacts [3]. Furthermore, oil spills could have critically negative effects on marine life, endangering the lives of seaweed (*Codium tomentosum*, *Codium barbata*), algae (*Ulva lactuca*), mollusks, (*Mytilus galloprovincialis*, *Ostrea edulis*, *Patella vulgata*), crustaceans (*Crangon crangon*) and fish (*Gobius niger*, *Solea*, *Trigla lucerna*) species [4].

A vast amount of research is found on the parameters of oil/water separation applications. Surface porosity and breakthrough pressure are considered the main parameters affecting the efficiency of membrane filters for oil/water separation applications [5]. Another study from Hazlett investigated and highlighted other main parameters such as surfactant concentration, fiber size and material, bed depth, packing density, water content, and continuous phase flow field velocity [6]. Bansal et al. [7] also investigated parameters such as droplet size, interfacial tension, inflow velocity, pressure drop, emulsion concentration, pore size, fiber fineness, permeability, and thickness.

Several technologies have been developed recently, including the air flotation, selective adsorptions, and filters (membranes) effective at oil/water separation and wastewater treatments [8]. Conventional methods also have been used worldwide for water/oil separation, such as burning, biodegradation via microorganisms, reduction of oil and water density differences, and evaporation of volatile components [9]. Rohrbach et al. [10] synthesized a hydrophilic and oleophobic cellulose-based filter with

* Corresponding author. Tel.: *+90 332 205 10 00*.
E-mail addresses*:* *kdogan@harran.edu.tr (K. Doğan), aliakbar.hussaini.1994@gmail.com (A.A. Hussaini), moerdal@erbakan.edu.tr (M.O. Erdal), muratyildirim@selcuk.edu.tr (M. Yıldırım)*
ORCID: 0000-0002-9770-8069 *(K. Doğan)*, 0000-0002-7128-9994 *(A.A. Hussaini)*, 0000-0003-4469-3438 *(M.O. Erdal)*, 0000-0002-4541-3752 *(M. Yıldırım)*
DOI: 10.35860/iarej.1075031

over 99% efficiency at 89.6 L/m^{2}h water flux. Wei et al. [11] have fabricated oxidized poly (arylene sulfide sulfone) (O-PASS) nanofibers via electrospinning. The obtained nanofiber exhibited significant hydrophobicity and 99% efficiency at high water flux 623.1 L/m^{2}h. In another study, Cheng et al. [12] have fabricated superhydrophobic nanofibers with separation efficiency of about 99.6% via coaxial electrospinning, containing polydimethylsiloxane (PDMS)/polyvinylidene fluoride (PVDF). Liu et al. [13] fabricated a water-repellent SiO_2 cotton fiber with a high oil-absorption capacity and adequate buoyancy. Shin & Chase [14] added a 1% mix of polyamide nanofibers to glass-fiber filter media, improving the separation efficiency to 84% from 71%. In addition, Secerov Sokolovic & Sokolović [15] investigated the effects of polyethylene, polyester, and polyurethane polymeric fibers on non-Brownian oil. Speth et al. [16] developed a new and scientifically based design method for fiber-bed coalescers. In another study, Shin & Chase [17] determined the effect of wettability on the coalescence mechanism.

Electrospinning is a simple, convenient and cost-effective technique for preparing separation membranes. Nanofibers are advantageous due to their large surface area, low energy consumption, and nanoscale-sized pores that are useful for achieving high separation efficiency [18]. A membrane with a large surface area can contact, adsorb, and coalesce a dispersed liquid [19]. Qiao et al. [20] produced polystyrene (PS)/polyacrylonitrile (PAN) sorbents with a high oil-absorption capacity using the electrospinning method. The oil absorption capacities (OAC) of PS/PAN sorbent in pump oil, peanut oil, diesel, and gasoline have been measured as 194.85, 131.7, 66.75 and 43.38 grams of oil per gram of absorbent (g/g), respectively. Zhu et al. [21] examined the oil/water selectivity and adsorption mechanism of polyvinyl chloride (PVC)/polystyrene (PS) electrospun fibers as sorbent materials. The PVC/PS nanofibers showed significant oil absorption capacities of 146, 119, 38 and 81 g/g for engine oil, peanut oil, diesel, and ethylene glycol, respectively.

This study produces nanofiber materials by adding ZnO, MoO_3, NiO, SiO_2, and TiO_2 to the PS/DMF solution. The morphological properties of the obtained nanofibers are characterized by scanning electron microscope (SEM), surface contact angle (CA) measurements, and fourier-transform infrared spectroscopy (FTIR) graphs. The resulting fiber surfaces were immersed in an oil/water emulsion to determine their oil absorption capacities.

2. Materials and Method

All chemicals (PS, ZnO, MoO_3, NiO, SiO_2 and TiO_2) were purchased from Sigma Aldrich. PS is added to the *N,N*-dimethyl formamide (DMF) solvent at a mass of 17% and mixed using a magnetic stirrer. After mixing for 30 minutes, a homogeneous 17% PS solution was obtained, after which the solution was loaded into a stainless-steel needle syringe with a diameter of 1.2 mm. With the unadulterated sample, nanoparticles were added at a weight-to-volume (w/v) ratio of 5% to the 17% polymer solution, and then the electrospinning process was performed. The electrospinning was carried out in a laboratory environment at room temperature. The voltage of 12-18 kV was applied, and the distance between the needle tip and the collector was 13-17 cm. In order to determine the oil absorption capacities (OAC) of the produced fibers, sunflower frying oil that was used repeatedly and supplied by a local cafeteria was added to the pure water at a ratio of 5 g/L and mixed.

By measuring the dry masses of fibers and their mass after absorbing oil, the oil absorption rates can be determined in two different ways. Firstly, it can be calculated by measuring the weights of the sorbents and oil using the following formula capacity (Equation 1) called as The gravimetric sorption capacity [22]:

$$\text{Absorbance capacity (\%)} = \frac{(m_{s,o} - m_s)}{m_s} \quad (1)$$

where m_s and $m_{s,o}$ are the sponge's masses before and after sorption. It can also be gained using the Equation (2):

$$\text{OAC} = \left[\frac{(W_3 - W_2 - W_4)}{\left(I - \frac{mc}{100}\right) W_1}\right] \quad (2)$$

where W_1 is the weight of the sample before the addition of oil in grams (g), W_2 is the weight of the syringe assembly (syringe chamber, filter paper, test tube, and sample in grams), W_3 is the weight of the syringe assembly after the centrifuge (syringe chamber, filter paper, test tube, sample, and absorbed oil in grams), W_4 is the weight of oil absorbed by the empty filter paper after the centrifuge in grams, and m_c is the initial moisture content of the sample [23].

3. Results

3.1. SEM Analysis

Electron microscope photos were taken under 15kV at a magnification of 5000X for all samples. Average fiber diameters were calculated from the SEM images. Average fiber diameters were calculated as 767 nm for the undoped sample and 760 nm, 1553 nm, 680 nm, 555nm, and 822 nm for samples doped respectively with ZnO, MoO_3, NiO, SiO_2, and TiO_2. A homogeneous distribution without the formation of a beaded structure in the fibers can be seen in Figure 1. These surface formations are thought to reduce the angle of contact.

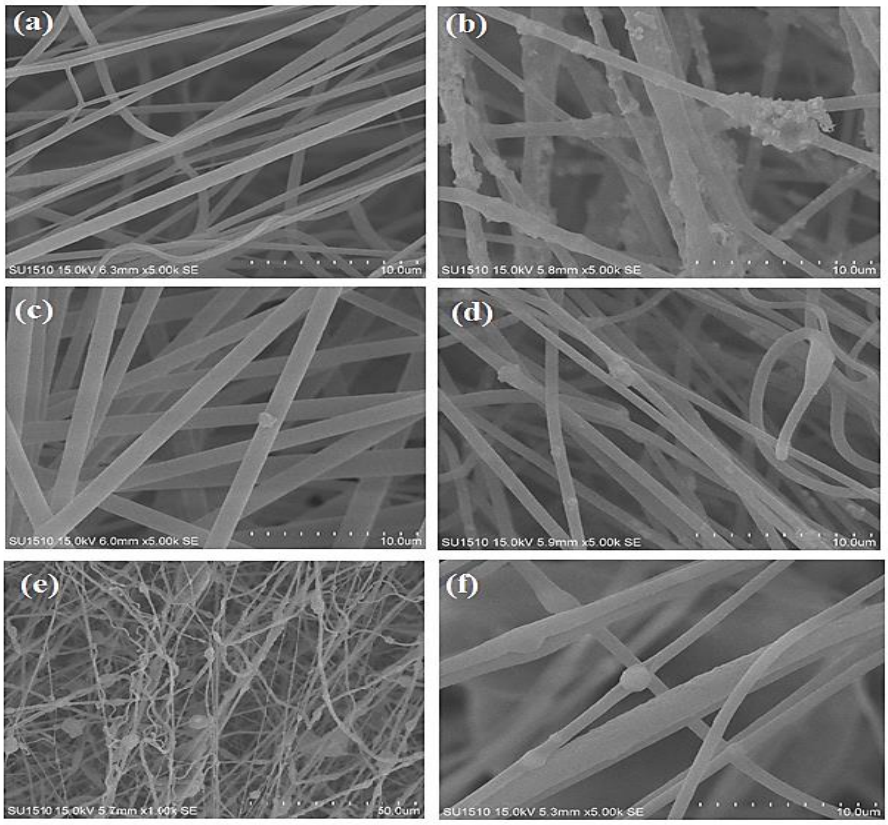

Figure 1. SEM images of a) Undoped PS, b) PS/ZnO, c) PS/MoO_3, d) PS/NiO, e) PS/SiO_2, and f) PS/TiO_2 nanofibers

In Figure 1e, the silicon dioxide particles significantly affected the fiber structure compared to the other doped samples. Although no beaded structures occurred, small lumps can be seen on all samples. In Figures 1c, 1d, and 1f, smooth surfaces were obtained as a result of the more homogeneous distribution of the additive in the solution, with lumps rarely being seen on the surface of the added fibers.

3.2. *Fourier-Transform Infrared Spectroscopy (FTIR) Analysis*

The chemical structure of the material is identified using FTIR. Figure 2 provides the FTIR diagrams obtained for the nanofibers containing 17% PS and 5% ZnO, MoO_3, NiO, SiO_2, or TiO_2 as an additive. Generally, CH_2, OH, and C=O bonds are typically observed above 1,500 cm^{-1}. Aromatic C-H bond vibrations were observed between 3050-3000 cm^{-1}. Moreover, aliphatic C-H absorptions were observed at 3000-2850 cm^{-1}. Meanwhile, peaks in the range of 1440-1610 cm^{-1} belong to the double bond voltage C=C in the aromatic ring. Peaks from the Si-O-Si bonds were seen at 1040-1060 cm^{-1}, and peaks evaluable as belonging to the O-Si-O bond were seen at 746-766 cm^{-1}. The peaks at 1450 cm^{-1} correspond to stretching in styrene ring [24]. The numerous peaks between 1030 and 548 cm^{-1} are due to CH deformation. The reference bands used are and the symmetric CH_2 stretching band at 2851 cm^{-1} for PS [25].

3.3. *Contact Angle (CA) Analysis*

Materials with a surface water contact angle greater than 90° are considered to be hydrophobic. A hydrophobic surface can easily be developed using building blocks with low surface energy or through surface modification [26]. Wettability is considered to be a true solid surface feature that defines the contact between a liquid and a solid surface and is often characterized using a liquid droplet contact angle (CA).

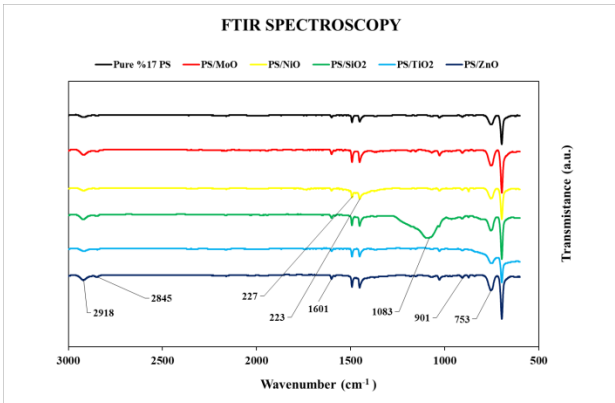

Figure 2. FTIR spectrums of the PS, PS/ZnO, PS/MoO_3, PS/NiO, PS/SiO_2 and PS/TiO_2 nanofibers

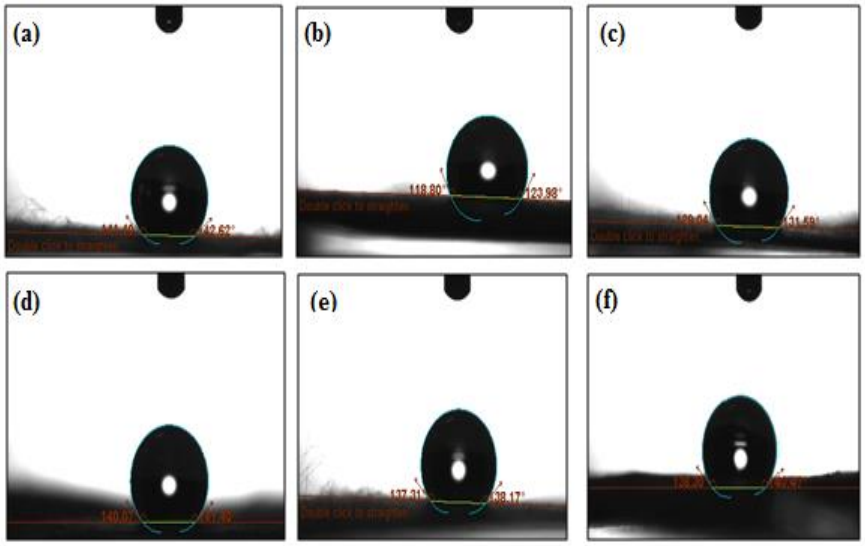

Figure 3. Contact angle measurements of a) undoped PS, b) PS/ZnO, c) PS/MoO_3, d) PS/NiO, e) PS/SiO_2, and f) PS/TiO_2

The wetness of the obtained nanofibers was determined via static water contact angle measurements. In order to measure the static water contact angle of deionized water (DI) on the obtained nanofibers, a goniometer was used. Deionized water was provided using a syringe pump (KDS Legato 100) and a stainless-steel needle (EFD, internal and external diameters of 250 and 520 um respectively) at a flow rate of 180 µL/hour. The contact angle was measured after resting the drop of deionized water on the PS nanofiber membrane for 5 seconds. All measurements and experiments were carried out in laboratory ambient conditions at room temperature. Contact angle measurements of the fibers are shown in Figure 3. The average static water contact angle was obtained from measurements taken in five different positions on the same sample. The contact angle graphs of the samples are shown Figure 4.

3.4. Oil Absorption Capacity Analysis

The obtained nanofibers were added to the ionized water as shown in Figure 4b. Samples were prepared by cutting 20×20 mm squares from the fabricated fibers and immersing them in the oil/water solution. It was carried out at room temperature. It was stirred in magnetic stirrer for 30 minutes at 500 rpm. The masses of the oil fibers were measured as shown in Figure 4c. The Oil carrying capacity (%) is calculated by the equation 1 and listed in Table 1. According to Table 1, the oil absorption capacity of unadulterated PS and the ZnO, MoO_3, NiO, SiO_2 and TiO_2-doped PS nanofibers were respectively measured as 68%, 24%, 103%, 70%, 114%, and 95% g/g. All the fabricated samples can be seen to have exhibited the potential to absorb oil and separate oil from water. The highest oil-carrying capacity is concluded to have been observed on the SiO_2 and MoO_3 doped fibers.

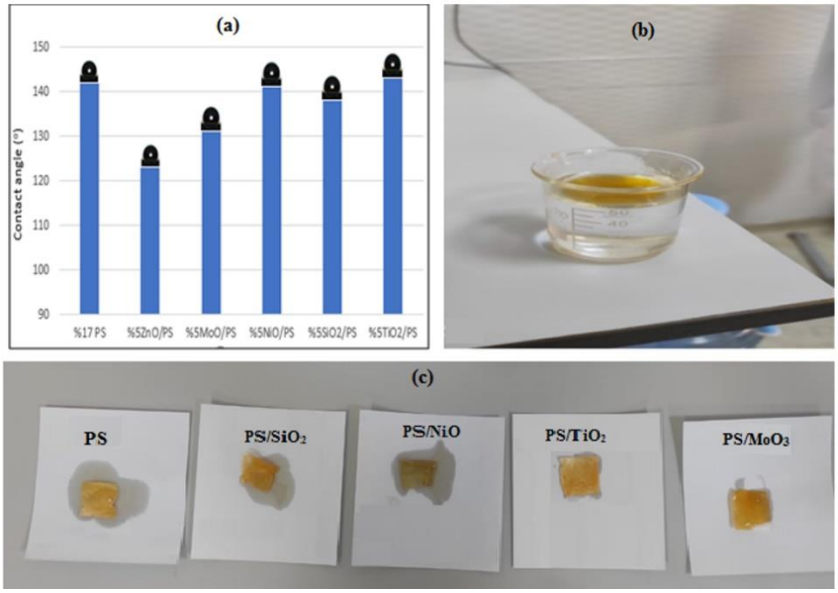

Figure 4. (a) Contact angle graphs of undoped PS, PS/ZnO, PS/MoO_3, PS/NiO, PS/SiO_2, and PS/TiO_2 nanofibers, (b) Oil absorption capacity measurement solution of fibers and (c) Oil absorption capacity of fibers after measurement

Table 1. Mass Measurements of the Waste Oil and Fiber Sample

Materials	Oil carrying capacity (%)	Water Contact Angle	References
PS/carbon nanotubes foam	98.4	161.2°	[27]
PS-SO3H/nylon	~100	158.0°	[28]
NTs/PS@AuNPs	99.4	145.0°	[29]
PMHS–TEOS-derived xerogel and PS	20.9	154.0°	[30]
polystyrene@Fe_3O_4 nanofiber	92-95	162.0°	[31]
PS-g-CNT	>99.94	152.0°	[32]
PS nanofiber	68	142.6°	This study
PS/ZnO nanofiber	24	123.9°	This study
PS/SiO_2 nanofiber	114	138.1°	This study
PS/NiO nanofiber	70	141.4°	This study
PS/MoO_3 nanofiber	103	131.5°	This study
PS/TiO_2 nanofiber	95	143.4°	This study

4. Conclusions

This study successfully fabricated PS/DMF nanofibers using the electrospinning method. ZnO, MoO_3, NiO, SiO_2, and TiO_2 nanoparticle additives were added to the nanofibers, and the resulting SEM, FTIR, and surface contact angle measurements of the produced nanofibers were examined in detail. According to the analysis results, the need for more studies can be concluded in order to optimize the contribution ratio to nanofibers. Regarding to SEM images, nanofibers have been distributed homogeneously without any beaded structure formation. Moreover, average fiber diameters are calculated as 767 nm for undoped sample and 760 nm, 1553 nm, 680 nm, 555 nm and 822 nm for ZnO, MoO_3, NiO, SiO_2 and TiO_2 doped samples, respectively.

In order to separate water using these nano-porous materials, nanofibers must have at least a 145^o surface contact angles with the water. However, the obtained results were found to be less than this value. Apart from the production method being the right choice, the PS/DMF ratio was also expected to have an effect on the desired contact angle values. In addition, although the added oxides were thought to have a hydrophobic effect, they did not exhibit the expected effect. The added particles were assumed would increase the expected effect of clinging to the outer surfaces of the nanofibers. However, the highest oil-carrying capacity is concluded to have been observed on the SiO_2 and MoO_3 doped fibers. In addition, no correlation was detected between the average fiber diameters and surface contact angle.

Declaration

The authors declared no potential conflicts of interest with respect to the research, authorship, and/or publication of this article. The authors also declared that this article is original, was prepared in accordance with international publication and research ethics, and ethical committee permission or any special permission is not required.

Author Contributions

K. Dogan and M.O. Erdal developed the methodology. K. Dogan performed the analysis. A.A. Hussaini and M. Yildirim wrote the manuscript. M. Yildirim and M.O. Erdal supervised and improved the study. All authors proofread the manuscript.

References

1. Galieriková, A., and M. Materna., *World Seaborne Trade One of Main Cause for Oil Spills?.* Transportation Research Procedia, 2020. **44**: p. 297–304.
2. Brussaard, C. P. D., Peperzak, L., Beggah, S., Wick, L. Y., Wuerz, B., Weber, J., Arey, J. S., Burg, B. Van Der, Jonas, A., Huisman, J., & Meer, J. R. Van Der., *Immediate ecotoxicological effects of short-lived oil spills on marine biota*. Nature Communications, 2016. **7**: p. 11206.
3. Cakir, E., Sevgili, C., and Fiskin, R., *Modelling of possible tanker accident oil spills in the Istanbul Strait in order to demonstrate the dispersion and toxic effects of oil pollution*. Transportation Research Part D: Transport and Environment, 2021. **90**: 102662.
4. Yildiz, S., Sönmez, V. Z., Sivri, N., Loughney, S., and Wang, J., *Modelling of possible tanker accident oil spills in the Istanbul Strait in order to demonstrate the dispersion and toxic effects of oil pollution*. Environ Monit Assess, 2021. **193**: 538.
5. Yue, X., Li, Z., Zhang, T., Yang, D., and Qiu, F., *Design and fabrication of superwetting fiber-based membranes for oil/water separation applications*. Chemical Engineering Journal, 2019. **364**: p. 292–309.
6. Hazlett, R.N., *Fibrous Bed Coalescence of Water Steps in the Coalescence Process*. Industrial & engineering chemistry fundamentals, 1969. **8**(4): p. 625–632.
7. Bansal, S., Arnim, V.V., Stegmaier, T., and Planck, H., *Effect of fibrous filter properties on the oil-in-water-emulsion separation and filtration performance*. Journal of

Hazardous Materials, 2011. **190**(1–3): p. 45–50.

8. Deng, D., Prendergast, D.P., MacFarlane, J., Bagatin, R., Stellacci, F., and Gschwend, P.M,. *Hydrophobic Meshes for Oil Spill Recovery Devices*. ACS Applied Material Interfaces, 2013. **5**(3): p. 774–781.
9. Kordjazi, S., Kamyab, K., and Hemmatinejad, N., *Super-hydrophilic/oleophobic chitosan/acrylamide hydrogel: an efficient water/oil separation filter*. Advanced Composites Hybrid Materials, 2020. **3**(2): p. 167–176.
10. Rohrbach, K., Li, Y., Zhu, H., Liu, Z., Dai, J., Andreasen, J., and Hu, L., *A cellulose based hydrophilic, oleophobic hydrated filter for water/oil separation*. Chemical Communication, 2014. **50**: p. 13296-13299.
11. Wei, Z., Lian, Y., Wang, X., Long, S., and Yang, J., *A novel high-durability oxidized poly (arylene sulfide sulfone) electrospun nanofibrous membrane for direct water-oil separation*. Separation and Purification Technology, 2020. **234**: 116012.
12. Cheng, XQ., Jiao, Y., Sun, Z., Yang, X., Cheng, Z., Bai, Q., Zhang, Y., Wang, k., and Shao, L., *Constructing Scalable Superhydrophobic Membranes for Ultrafast Water–Oil Separation*. ACS Nano, 2021. **15**(2): p. 3500–3508.
13. Liu, F., Ma, M., Zang, D., Gao, Z., and Wang, C., *Fabrication of superhydrophobic/superoleophilic cotton for application in the field of water/oil separation*. Carbohydrate Polymers, 2014. **103**: p. 480–487.
14. Shin, C., and Chase, G.G., *Separation of Water-in-Oil Emulsions Using Glass Fiber Media Augmented with Polymer Nanofibers*. Journal of Dispersion Science and Technology, 2006. **27**(4): p. 517-522.
15. Sokolović, RMŠ., and Sokolović, SM., *Effect of the Nature of Different Polymeric Fibers on Steady-State Bed Coalescence of an Oil-in-Water Emulsion*. Industrial & engineering chemistry research, 2004. **43**(20): p. 6490–6495.
16. Speth, H., Pfennig, A., Chatterjee, M., and Franken, H., *Coalescence of secondary dispersions in fiber beds*. Separation and purification technology, 2002. **29**(2): p. 113-119.
17. Shin, C., and Chase, G., *The effect of wettability on drop attachment to glass rods*. Journal of colloid and interface science, 2004. **272**(1): p. 186–190.
18. Fan, L., Yan, J., He, H., Deng, N., Zhao, Y., Kang, W., and Cheng, B., *Electro-blown spun PS/PAN fibrous membrane for highly efficient oil/water separation*. Fibers and Polymers, 2017. **18**(10): 1988-1994.
19. Shin, C., and Chase, GG., *Water-in-Oil Coalescence in Micro-Nanofiber Composite Filters*. AIChE journal, 2004. **50**(2): p. 343-350.
20. Qiao, Y., Zhao, L., Li, P., Sun, H., and Li, S., *Electrospun polystyrene/polyacrylonitrile fiber with high oil sorption capacity*. Journal of Reinforced Plastics and Composites, 2014. **33**(20): p. 1849-1858.
21. Zhu, H., Qiu, S., Jiang, W., Wu, D., and Zhang, C., *Evaluation of Electrospun Polyvinyl Chloride/Polystyrene Fibers As Sorbent Materials for Oil Spill Cleanup*. Environmental science & technology, 2011. **45**(10): p. 4527-4531.
22. Pham, VH., and Dickerson, JH., *Superhydrophobic Silanized Melamine Sponges as High Efficiency Oil Absorbent Materials*. ACS applied materials & interfaces, 2014. **6**(16): p. 14181-14188.
23. Wang, N., Maximiuk, L., Fenn, D., Nickerson, MT., Hou, A., *Development of a method for determining oil absorption capacity in pulse flours and protein materials*. Cereal Chemistry, 2020. **97**(6): p. 1111-1117.
24. George, G., and Anandhan, S., *Glass fiber–supported NiO nanofiber webs for reduction of CO and hydrocarbon emissions from diesel engine exhaust*. Journal of Materials Research, 2014. **29**(20): p. 2451-2465.
25. Mylläri, V., Ruoko, T-P., Syrjälä, S., *A comparison of rheology and FTIR in the study of polypropylene and polystyrene photodegradation*. Journal of Applied Polymer Science, 2015. **132**(28): 42246.
26. Ma, W., Zhang, Q., Hua, D., Xiong, R., Zhao, J., Rao, W., Huang, S., Zhan, X., Chen, F. and Huang, C., *Electrospun fibers for oil-water separation*. Rsc Advances, 2016. **6**(16): p. 12868-12884.
27. Shan, W., Du, J., Yang, K., Ren, T., Wan, D., and Pu, H., *Superhydrophobic and superoleophilic polystyrene/carbon nanotubes foam for oil/water separation*. Journal of Environmental Chemical Engineering, 2021. **9**(5): p. 106038.
28. Wang, L., Zhang, J., Wang, S., Yu, J., Hu, W., and Jiao, F., *Preparation of a polystyrene-based super-hydrophilic mesh and evaluation of its oil/water separation performance*. Journal of Membrane Science, 2020. **597**: p. 117747.
29. Zhang, L., Gu, J., Song, L., Chen, L., Huang, Y., Zhang, J., and Chen, T., *Underwater superoleophobic carbon nanotubes/core–shell polystyrene@Au nanoparticles composite membrane for flow-through catalytic decomposition and oil/water separation*. Journal of Materials Chemistry A, 2016. **4**(28): 10810-10815.
30. Guo, P., Zhai, S-R., Xiao, Z-Y., Zhang, F., An, Q-D., Song, X-W., *Preparation of superhydrophobic materials for oil/water separation and oil absorption using PMHS–TEOS-derived xerogel and polystyrene*. Journal of sol-gel science and technology, 2014. **72**(2): p. 385-393.
31. Moatmed, SM., Khedr, MH., El-dek, SI., Kim, H-Y., and El-Deen, AG., *Highly efficient and reusable superhydrophobic/superoleophilic polystyrene@ Fe3O4 nanofiber membrane for high-performance oil/water separation*. Journal of Environmental Chemical Engineering, 2019. **7**(6): p. 103508.
32. Gu, J., Xiao, P., Chen, J., Liu, F., Huang, Y., Li, G., ... & Chen, T. *Robust preparation of superhydrophobic polymer/carbon nanotube hybrid membranes for highly effective removal of oils and separation of water-in-oil emulsions*. Journal of Materials Chemistry A, 2014. **2**(37): p. 15268-15272.